The Journal of Neuroscience, November 1, 1999, *19*(21):9374–9384

Targeted Expression of Truncated *Glued* Disrupts Giant Fiber Synapse Formation in *Drosophila*

Marcus J. Allen,[1] Xiaoliang Shan,[1] Phyllis Caruccio,[1] Stephan J. Froggett,[1] Kevin G. Moffat,[2] and R. K. Murphey[1]

[1]*Department of Biology, Morrill Science Center, University of Massachusetts, Amherst, Massachusetts 01003, and* [2]*Department of Biological Sciences, University of Warwick, Coventry CV4 7AL, United Kingdom*

Glued[1] (*Gl*[1]) mutants produce a truncated protein that acts as a poison subunit and disables the cytoplasmic retrograde motor dynein. Heterozygous mutants have axonal defects in the adult eye and the nervous system. Here we show that selective expression of the poison subunit in neurons of the giant fiber (GF) system disrupts synaptogenesis between the GF and one of its targets, the tergotrochanteral motorneuron (TTMn). Growth and pathfinding by the GF axon and the TTMn dendrite are normal, but the terminal of the GF axon fails to develop normally and becomes swollen with large vesicles. This is a presynaptic defect because expression of truncated *Glued* restricted to the GF results in the same defect. When tested electrophysiologically, the flies with abnormal axons show a weakened or absent GF–TTMn connection. In *Glued*[1] heterozygotes, GF–TTMn synapse formation appears morphologically normal, but adult flies show abnormal responses to repetitive stimuli. This physiological effect is also observed when tetanus toxin is expressed in the GFs. Because the GF–TTMn is thought to be a mixed electrochemical synapse, the results show that Glued has a role in assembling both the chemical and electrical components. We speculate that disrupting transport of a retrograde signal disrupts synapse formation and maturation.

Key words: retrograde motors; transport; p150^{GLUED}*; giant fibers; UAS–GAL4; dynein–dynactin*

Neurons are long, polarized cells that rely extensively on the cytoskeleton for relaying information and subcellular constituents to and from the soma and distal processes. Anterograde-directed transport along the microtubules is conducted by the kinesin family of motors and retrograde-directed transport is conducted primarily by cytoplasmic dynein (for review, see Hirokawa, 1998). In *Drosophila*, kinesin mutations alter anterograde transport and cause organelle jams in larval axons that disrupt synaptic function and cause behavioral and physiological abnormalities (Gho et al., 1992; Hurd and Saxton, 1996; Hurd et al., 1996; Gindhart et al., 1998). Similarly, mutations that affect dynein–dynactin function disrupt retrograde transport and cause axonal defects and synaptic dysfunction (Phillis et al., 1996; Reddy et al., 1997; Murphey et al., 1999).

One hypothesis for the dynein–dynactin defects is that the retrograde motor plays an important role in the formation or stability of certain synapses (Riccio et al., 1997; Murphey et al., 1999). The *Glued* locus encodes a 150 kDa protein that is part of dynactin, a protein complex that activates cytoplasmic dynein (Waterman-Storer and Holzbaur, 1996; Holleran et al., 1998) and links the motor to its cargo (Karki and Holzbaur, 1995; Vaughan and Vallee, 1995; Waterman-Storer et al., 1997). The dominant *Glued*[1] (*Gl*[1]) mutation in *Drosophila* results in a truncated protein product (Swaroop et al., 1985), which competes with wild-type protein, forming complexes that can bind to dynein but are unable to bind to the cargo, and this disrupts retrograde transport (McGrail et al., 1995; for review, see Allan, 1996).

To examine the role of retrograde motors in synaptogenesis, we have examined the giant fiber (GF) system of *Drosophila*, a simple circuit with a single large central synapse amenable to electrophysiological studies (for review, see Thomas and Wyman 1983). The GFs relay excitation from the brain to the thoracic ganglia where they make two identified synapses: one to the large tergotrochanteral motorneuron (TTMn) that drives the leg extensor muscle (TTM) and a second with the peripherally synapsing interneuron (PSI), which then synapses with the dorsal longitudinal flight motoneurons (DLMns) (King and Wyman, 1980).

Here we show, by selectively expressing a truncated Glued poison subunit in the neurons of the giant fiber system (Brand and Perrimon, 1993; Phelan et al., 1996; Allen et al., 1998), that the retrograde motor is needed to generate a normal GF–TTMn synapse and that the effects are specific to the GF. Morphologically, the GF in transgenic animals fails to assemble the normal presynaptic terminal. Testing of the GF–TTMn synapse electrophysiologically reveals weakened or absent connections that often show no dye coupling. The physiological phenotypes observed in mutant and transgenic flies are mimicked when chemical transmission is blocked by targeted expression of the tetanus toxin light chain in the GF. This supports recent evidence that the synapse is a mixed electrochemical junction. Our data show that both the electrical and chemical components are compromised by disruption of the retrograde motor. These results support a model in which a retrograde signal received by the GF enables synapse maturation to proceed.

MATERIALS AND METHODS

Drosophila *stocks.* All stocks were grown at 25°C or room temperature on standard medium. Two P[GAL]4 lines that expressed in the giant

Received June 4, 1999; revised Aug. 9, 1999; accepted Aug. 13, 1999.

This work was supported by grants to R.K.M. from National Institutes of Health (NS15571) and the National Science Foundation (IBN 9514701). We thank Dr. Randall Phyllis, Dr. Ulrich Thomas, and Dan Osuch for comments on this manuscript. The UAS–tetanus toxin flies were kindly provided by Dr. Sean Sweeney (University of Cambridge).

Correspondence should be addressed to Dr. Marcus J. Allen, Department of Biology, Morrill Science Center, University of Massachusetts, Amherst, MA 01003. E-mail: mjallen@bio.umass.edu.

fiber system were used: P[GAL4] A307 (Phelan et al., 1996; Allen et al., 1998), hereafter referred to as A307, an enhancer line that shows expression in the GF, the TTMn, the PSI, and possibly other neurons in the giant fiber system (e.g., the DLMns). The other line, P[GAL4] c17, hereafter referred to as c17, shows expression in the GF and a subset of sensory neurons (Trimarchi et al., 1999) but in no other identified neurons of the giant fiber system. For developmental analysis, the *In(2LR)GlaBc* chromosome was used so that pupae that contained only A307 could be distinguished from those carrying A307 and P[UAS–$Gl^{\Delta 96B}$].

Generation of the P[UAS–Gl^{Δ}] lines. The 2897 bp truncated cDNA, encoding only the N-terminal 922 amino acids of Glued (Fan and Ready, 1997), was removed from pCaSpeR-hs (DNA kindly provided by Dr. Don Ready, Purdue University) as an *Eco*RI fragment and cloned into the pUAST vector (Brand and Perrimon, 1993). Transgenic lines containing this construct were generated by germline transformation of w^{1118} embryos essentially as described by Spradling and Rubin (1983). Twelve independent transformant lines were generated, of which two, both second chromosome viable insertions (UAS–$Gl^{\Delta 84}$ and UAS–$Gl^{\Delta 96B}$), were used in this study.

Immunocytochemistry. CNS of adults and pupae were dissected in 100 mM phosphate buffer (PB) and immediately fixed in 4% paraformaldehyde in PB for at least 30 min at room temperature. Preparations were washed twice in PB + 0.4% Triton X-100 (PBT), treated with 2N HCl in PBT for 30 min, and further washed four times to remove the acid. After it was blocked for 2 hr in 100 mM PB, 1% bovine serum albumin, 0.1% Triton X-100 (PAT), the tissue was incubated overnight with a rabbit polyclonal anti-β-galactosidase antibody (Cappel, Tunhout, Belgium) at a dilution of 1:10,000 in PAT + 3% normal goat serum. Preparations were then washed at least three times (1 hr each time) in PAT before they were incubated with a biotinylated goat anti-rabbit secondary antibody (Vector Labs, Burlingame, CA), 1:250 in PAT. Further processing was performed according to ABC kit instructions (Vector Labs), and the specimens were dehydrated through a series of ethanol dilutions, cleared using methyl salicylate, and mounted in Canada Balsam. Selected whole-mount preparations were embedded in plastic as described by Murphey et al. (1999) and sectioned in the horizontal plane at 7 μm thickness.

Physiology. Adult flies were prepared in a method similar to that described by Tanouye and Wyman (1980) and Gorczyca and Hall (1984). Flies were lightly anesthetized with ether and waxed, ventral side down, onto a small podium in a Petri dish. The wings were waxed down in an outward position to expose the dorsal and lateral surfaces of the thorax. The GFs were activated extracellularly by two etched tungsten electrodes, one placed through each eye into the supra-esophageal ganglion. Threshold for the short-latency direct excitation for GF stimulation was usually a pulse of ~10–20 V for 0.03 msec from a Grass S44 stimulator (Grass Instruments, Quincy, MA) (Tanouye and Wyman, 1980; Engel and Wu, 1996). We therefore routinely gave pulses two to three times threshold to ensure that threshold was always exceeded. For direct extracellular stimulation of the motoneurons the tungsten electrodes were placed in the thoracic ganglion. A tungsten electrode placed in the abdominal cavity served as a ground.

Intracellular recordings from muscles were obtained with saline-filled glass micropipettes (resistance 40–60 MΩ) driven through the cuticle into the muscle fibers. Intracellular recordings were amplified using a Getting 5A amplifier (Getting Instruments, Iowa City, IA) and recordings observed and photographed directly from a storage oscilloscope (Tektronics, Wilsonville, OR).

Our method of activating the GFs by brain stimulation raises the concern that other neurons, involved in descending pathways that lead to the muscles, are also being activated. However, some experimental preparations gave no response in either TTM or DLM on brain stimulation (see Results), indicating that there are no alternative pathways that can be activated with our method of brain stimulation. Stimulation of the thorax in these unresponsive preparations led to short-latency muscle responses and demonstrated that the motoneurons and neuromuscular junctions were intact.

Each animal was subjected to three standard tests: response latency, refractory period, and following frequency. For latencies each fly was given five single pulses that were overlaid on the storage oscilloscope. Measurements were taken from the beginning of the stimulation artifact to the beginning of the EPSP. In cases where the five pulses did not give identical response latencies, the shortest latency was always measured. To determine the refractory period, twin pulses were used at 10, 8, 6, 4, 3, and 2 msec apart. The refractory period was recorded as the shortest of these intervals at which a second response was always seen and therefore always an integer. For following frequency, stimuli were given at 250 Hz, a frequency at which the TTM will follow perfectly and the DLM will start to fail (Tanouye and Wyman, 1980). The number of responses to 10 stimuli was counted and expressed as a percentage. In some experiments for measurements of following at different frequencies, each animal was given 10 pulses from a Grass S48 stimulator at each of the three frequencies: 100, 200, and 300 Hz. The signals were amplified using a Getting 5A microelectrode amplifier and stored on a PC with pCLAMP software and a DMA interface board (Axon Instruments, Foster City, CA). Analysis was performed on the PC using pCLAMP and Exel 97 software (Microsoft, Redmond, WA).

Retrograde staining of motoneurons. To stain motor neurons using neurobiotin, a technique similar to that of Trimarchi and Schneiderman (1994) and Trimarchi and Murphey (1997) was used. Distilled water (25 μl) was added to 0.1 mg of neurobiotin powder, and a 2–4 μl drop was placed on a slide. As it dried, a tungsten probe was pulled along the edge of the drop, coating the tip with crystals by capillary action. This was repeated with a second drop for all probes. Flies were anesthetized using ether and waxed to a slide, and an etched tungsten wire was used to poke a small hole in the cuticle at the point of TTM attachment. The coated probe was then used to apply crystals to the underlying muscle. Flies were then incubated in a moist chamber for 15–20 min at room temperature to allow dye uptake.

After incubation the flies were partially dissected by removing the legs at the base of the coxa, head, and abdomen and fixed over night in 4% paraformaldehyde at 4°C. The thoracic ganglia were removed and rinsed three to four times in 0.1 M PB. The ganglia were then washed in PBT for 2–3 hr at room temperature and in 100 mM PB for 15 min. Visualization of the staining was achieved using an ABC kit (Vector Labs). A variation of the J. Adams intensification method for 3,3′-diaminobenzidine-tetrahydrochloride (DAB) (Adams, 1981) was used in which 10 mg of DAB (Sigma, St. Louis, MO) was dissolved in 20 ml of 100 mM PB to which 0.5 ml of 1% $CoCl_2$ and 0.4 ml of 1% nickel ammonium sulfate $Ni(NH_2)(SO_4)_2$ were added. The solution was filtered and diluted 1:3 with 100 mM PB, and the ganglia were incubated for 3 min, then washed briefly in 0.1 M PB. The ganglia were then further incubated in DAB (0.3 mg/ml 0.1 M PB) with 0.3% H_2O_2 for 6–10 min, rinsed in 0.1 M PB, dehydrated through an ethanol series, cleared in methylsalicylate, and mounted in Canada balsam.

Preparations were scored initially for heavy TTMn staining and those that showed suitable staining were further scored twice independently (one blind) for staining of the GFs. The results were then combined to produce Table 2 (see Results).

Image capturing and processing. Images in several focal planes were captured from whole-mount CNS preparations using a SPOT digital camera (Diagnostic Instruments, Sterling Heights, MI) and imported into Adobe Photoshop 5.0 software (Adobe Systems, San Jose, CA) on an Apple Macintosh G3 computer. Montages were then constructed using the "clone tool" showing axonal projections that cross several planes of focus in a single image. For the sectioned preparation, an image of the relevant single section was captured using the SPOT camera.

RESULTS

Overexpression of truncated *Glued* (Gl^{Δ}) in the giant fiber system causes aberrant GF morphology

To selectively disrupt the dynein–dynactin complex in the giant fiber system, we assembled a UAS–Gl^{Δ} construct, by cloning a truncated *Glued* cDNA into the pUAST vector. This truncated transgene produces a "poison" protein product like that produced by the Gl^{1} mutation (Fan and Ready, 1997). Once introduced into flies by P element-mediated transformation (see Materials and Methods), we then used the GAL4–UAS system of Brand and Perrimon (1993) to achieve selective expression. We used eye-specific GAL4 activators as an initial test for transgene function. Crosses of *sev*–GAL4 (Basler et al., 1989) and GMR–GAL4 (Freeman, 1996) to two independent UAS–Gl^{Δ} lines resulted in progeny with reduced and rough eyes (data not shown). These eye phenotypes were similar to disruptions in ommatidial formation and array seen in Gl^{1}/+ mutants (Harte and Kankel, 1983; Fan and Ready, 1997). Interestingly, the progeny from the GMR–

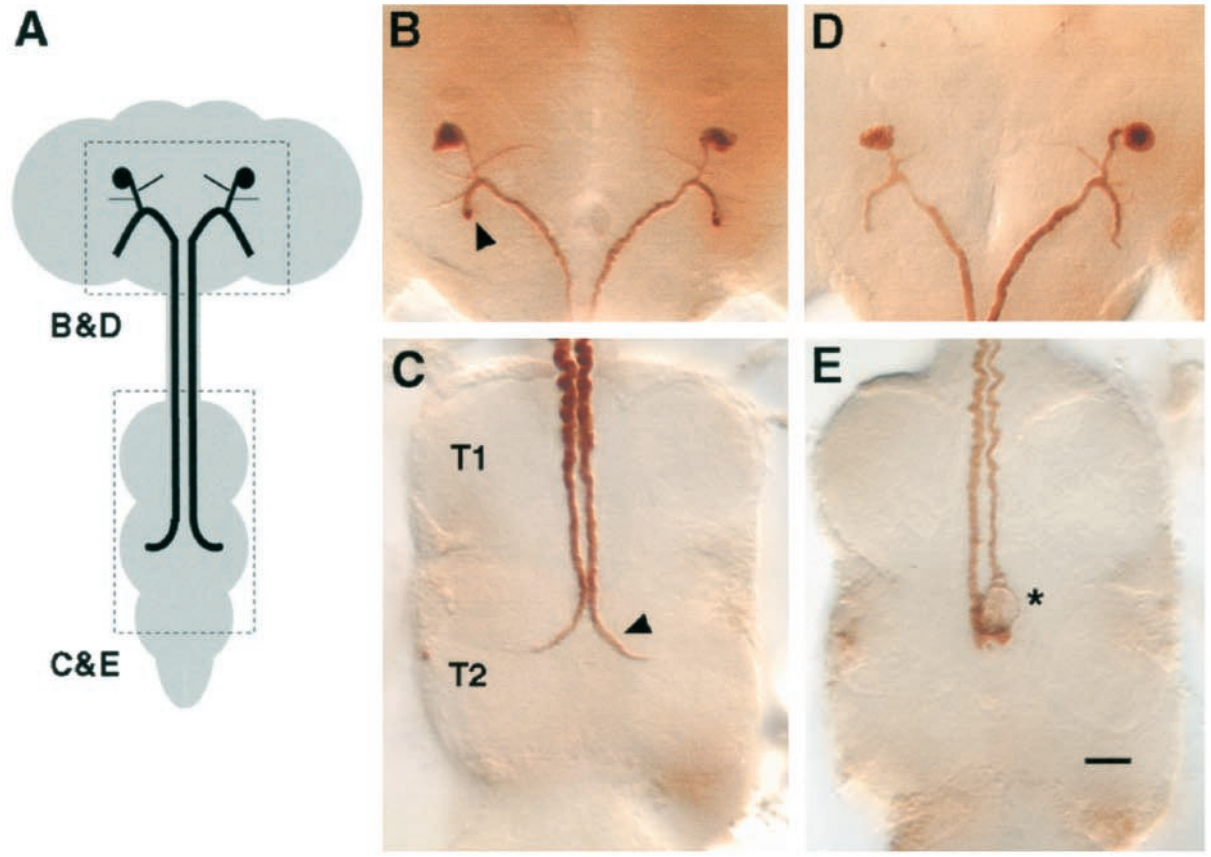
A
B&D
C&E
B
D
C
T1
T2
E
*

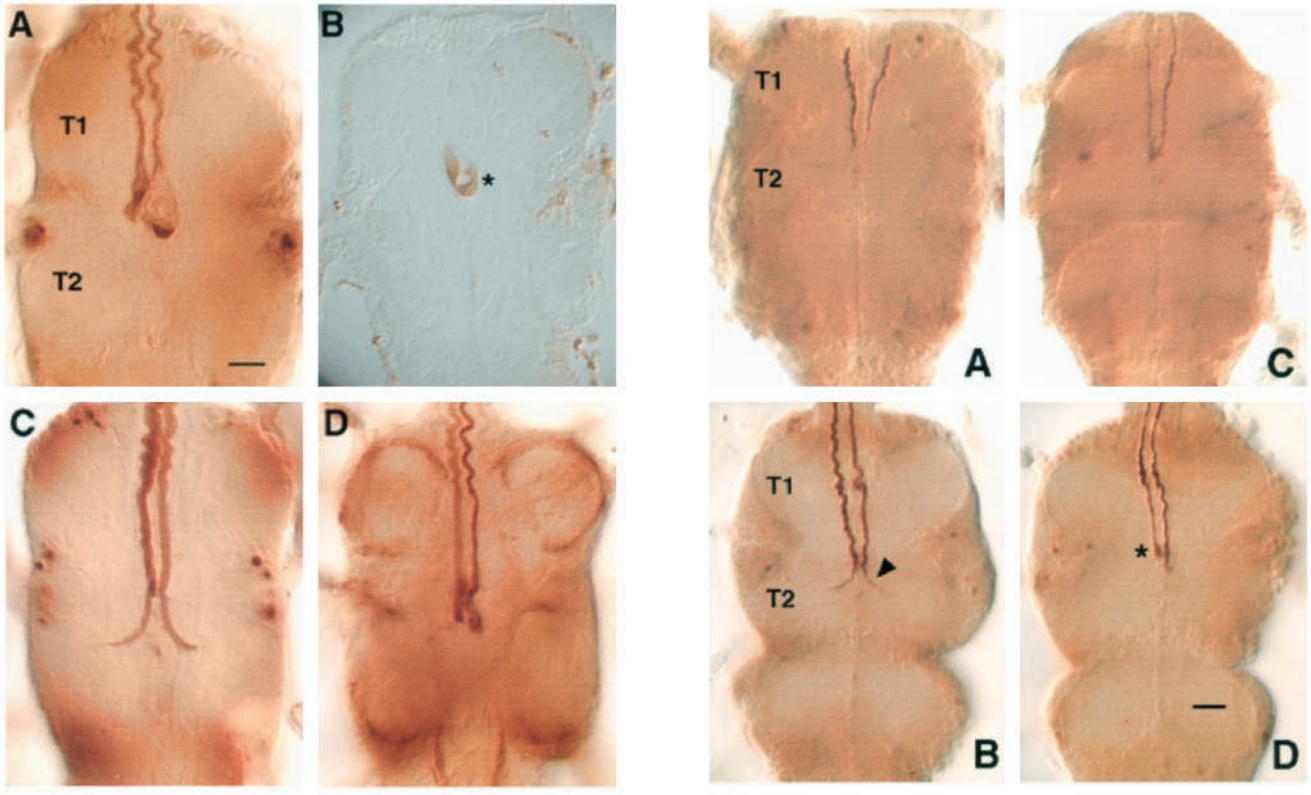
A
T1
T2
B
*
C
D
T1
T2
A
C
T1
T2
B
*
D

GAL4 cross showed a more severe disruption in eye formation than Gl^1/+ heterozygotes, indicating that we could increase the dosage of poison subunit above that of the heterozygous mutant flies.

To examine neural defects we expressed the truncated transgene with GF-specific GAL4 activators. We used the previously characterized enhancer-trap A307 to express Gl^Δ in neurons of the giant fiber system. This P[GAL4] insert drives expression in the GF and TTMn, before they make their synaptic connection, and has been used to follow the development of the giant fiber system (Phelan et al., 1996; Allen et al., 1998). In wild-type specimens, the adult GFs are seen as large bilaterally symmetrical neurons that project from the brain to the thoracic ganglia (Fig. 1*A*). Each soma can be visualized near the dorsal surface of the brain; a thin neurite extends posteriorly and ventrally from the cell body to the axon and dendritic field. The largest dendritic branch is the posterior lateral dendrite (Fig. 1*B*, *arrowhead*), and other, smaller processes can be seen, including a dorsal medial branch that projects into the giant commissural interneurons [J. A. Drummond, M. J. Allen, K. G. Moffat (1997) P[GAL4]-307 enhancer-trap pattern. Flybrain on-line: http://www.flybrain.org. Accession number AA00098]. The axon projects posteromedially and runs dorsally through the cervical connective into the thoracic ganglion and passes through the prothoracic neuromere (T1) and into the mesothoracic neuromere (T2), where it dives ventrally and bends laterally (Fig. 1*C*, *arrowhead*). It is along this distinctive bend that synaptic contact with the large TTMn is made (Thomas and Wyman, 1982; Blagburn et al., 1999).

Overexpression of the Gl^Δ in neurons of the giant fiber system resulted in GFs that failed to show their characteristic bends in the second thoracic neuromere, and their axons had swellings at the terminals (Fig. 1*E*). Flies carrying A307 and a UAS–*lacZ* reporter construct were crossed to two independent UAS–Gl^Δ lines (UAS–$Gl^{\Delta 84}$ and UAS–$Gl^{\Delta 96B}$), and the adult GF morphology was examined by immunocytochemistry. In both cases the GFs showed the same phenotype (Figs. 1*E*, 2*A*, Table 1). The bilaterally paired GF axons project into T2 where they would normally meet their target neurons, but they do not show the lateral bend. Instead the GF axons show terminal swellings of up to three times the normal axon diameter. This abnormal morphology was seen in >90% of preparations (Table 1). Light microscopic sections through these axons show that they are distorted by large vesicles that exclude the LacZ marker (Fig. 2*B*). Arborization of the dendritic field, however, appears to be unaffected by Gl^Δ expression (Fig. 1*D*).

In the GAL4–UAS system the poison subunit is expressed in a background that contains two wild-type *Glued* alleles. We therefore looked at *Glued* ^{1} mutants in which every cell contains one copy of the gene that synthesizes the poison subunit and another that produces wild-type protein. Interestingly, Gl^1/+ heterozygotes show normal GF morphology (Fig. 2*C*, Table 1); therefore the dosage of mutant protein in these flies results in normal, wild-type axon morphology.

Table 1. Occurrence of anatomical defects in GF axons

Genotype	GFs examined[a]	% with abnormal morphology
Controls[b]	89	0
UAS–*lacZ*; A307/UAS–$Gl^{\Delta 84}$	68	98.5
w; c17,UAS–*lacZ*/UAS–$Gl^{\Delta 84}$	41	92.7
UAS–*lacZ*; A307/UAS–$Gl^{\Delta 96B}$	66	100
w; c17,UAS–*lacZ*/UAS–$Gl^{\Delta 96B}$	11	100
UAS–*lacZ*; A307; Gl^1/*TM6B*	48	2

[a]Each GF was scored individually. In most preparations, two axons clearly stained and were scored accordingly; however, occasionally only one GF could be scored with confidence.

[b]Animals that contained either A307 or c17 with a UAS–*lacZ* reporter construct.

When Gl^Δ was targeted to the presynaptic cell the axon was disrupted

Because A307 expresses in both the GF and TTMn, we could not determine the site of the defects. To test whether the effect on the GF presynaptic terminal was caused by disrupting Glued function in the presynaptic or both presynaptic and postsynaptic cells, a second P[GAL4] line (c17) that expresses in the GF but not the TTMn was used. This line shows weaker expression in the GF than A307 when comparing the level of α-LacZ antibody staining seen in preparations processed in parallel. In the c17 enhancer-trap reporter protein (LacZ) could be detected in the GF as early as 24 hr after puparium formation (APF) if overstained, but expression was never seen in the TTMn. These c17 flies were crossed to the two UAS–Gl^Δ lines (UAS–$Gl^{\Delta 84}$ and UAS–$Gl^{\Delta 96B}$), and the GFs in these animals were examined. The GFs did not show the characteristic lateral bends and were often swollen at the distal tips of the axons (Table 1). The defects in these c17 flies often appeared less severe than those seen with A307 (Fig. 2, compare *A* and *D*), consistent with the presumed strength of expression. In summary, expression of UAS–Gl^Δ in the GF alone disrupts synaptogenesis.

←

Figure 1. **Top.** Expression of Gl^Δ disrupts axon morphology in the GFs. *A*, Diagram depicting the morphology of the GFs in the CNS. *Boxes* indicate regions of the brain and thoracic ganglia shown in *B–E*. The soma and dendrites are located in the brain (*box* labeled *B&D*). The axon and presynaptic terminal are located in the second thoracic segment (*box* labeled *C&E*). *B*, *C*, Whole-mount preparations of the CNS from UAS–*lacZ*; A307 adult flies. Immunocytochemistry has revealed LacZ reporter protein in the GFs in the brain, including the cell bodies and the dendritic field (*B*), and in the thoracic ganglia where the GFs show their distinctive bends in the mesothoracic neuromere (*C*, *arrowhead*). *D*, *E*, Whole-mount preparations of the CNS from UAS–*lacZ*; A307/UAS–Gl^Δ adult flies. The dendritic field is unaffected by Gl^Δ (*D*); however, the axon terminals exhibit large swellings and no bend (*E, asterisk*). Scale bar, 20 μm.

Figure 2. **Left.** Disruptions in axon morphology are dependent on the dose of poison subunit. *A*, Whole-mount adult thoracic ganglia from UAS–*lacZ*; A307/UAS–$Gl^{\Delta 96B}$ showing large terminal axon swellings. *B*, A 7 μm horizontal section through a UAS–*lacZ*; A307/UAS–$Gl^{\Delta 96B}$ adult thoracic ganglia showing a large vesicle devoid of reporter protein within the swelling (*asterisk*). *C*, Adult thoracic ganglia from UAS–*lacZ*; A307; Gl^1/+ showing normal GF morphology. *D*, Whole-mount adult thoracic ganglia from c17, UAS–*lacZ*/UAS–Gl^Δ showing lack of GF bending but less severe swelling than seen in *A*. Scale bar, 20 μm.

Figure 3. **Right.** Developmental analysis of mutant and wild-type giant fibers. *A, B*, Dorsal views of whole-mounted pupal thoracic nervous systems from control flies at 24 and 48 hr APF, respectively. Note the distinctive terminal bends in the mesothoracic neuromere (*T2*) seen at 48 hr (*B*, *arrowhead*). *C, D*, Dorsal views of whole-mounted pupal thoracic nervous systems from flies expressing Gl^Δ in the GFs at 24 and 48 hr APF, respectively. These mutant axons show no bends at 48 hr, and small swellings can be seen at the axon tips (*D*, *asterisk*). Scale bar, 20 μm.

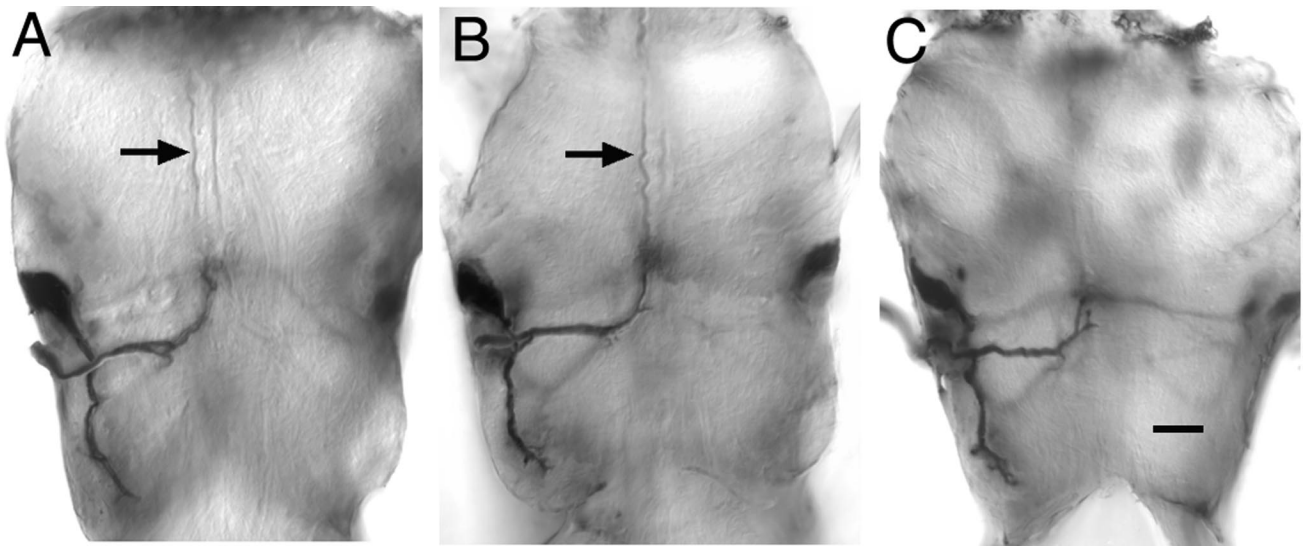

Figure 4. The strength of dye coupling is affected by the truncated Glued protein. *A*, Iontophoresis of neurobiotin into the TTM often led to dye filling of the GF in the Gl^1/+ heterozygotes (*arrow*) just as is seen in the wild-type animals (Table 3). *B*, Expression of the truncated subunit under the control of c17 had no detectable effect on dye coupling to the GF. *C*, Many fewer specimens showed dye coupling to the GF when the truncated Glued was expressed under the control of A307. See also Table 3. Scale bar, 20 μm.

Defects occur late in GF development

To understand the emergence of the defects in the GFs, we examined the GF at various stages of metamorphosis. We dissected the CNS from various pupal stages of A307; UAS–$Gl^{\Delta 96B}$ flies as well as from controls that contained only the enhancer-trap and the UAS–*lacZ* reporter construct. At 24 hr APF, the GFs have grown through the brain down the connective into the thoracic ganglia and reached the midpoint of T2 (Allen et al., 1998). Both controls and experimental preparations show GFs at the midpoint of T2 at 24 hr APF, but no difference is seen between controls and experimentals (Fig. 3*A*,*C*). This indicates that growth and pathfinding in the brain and connective are unaffected by Gl^{Δ}. At 48 hr APF (P7) (Bainbridge and Bownes, 1981), control GFs show the characteristic bends (Fig. 3*B*) and are in contact with the TTMn (Phelan et al., 1996; Allen et al., 1998). However, experimental GFs expressing $Gl^{\Delta 96B}$ remain at the midpoint of T2 and show no terminal bends. In addition, small swellings can be seen at the tips of the axons (Fig. 3*D*, *arrowhead*). At 72 hr APF (P9–10) (Bainbridge and Bownes, 1981), all control preparations that were examined show bends, and experimental axons show no bends, but small swellings similar to those seen at 48 hr APF are present (data not shown). During the remainder of pupal development, the GFs increase to their adult diameter of ~7 μm (Fig. 1*B*). In axons expressing $Gl^{\Delta 96B}$, the swellings increase markedly in size to give bulbs axon diameters that were several times the normal size (Figs. 1*D*, 2*A*). The dendritic fields of the experimental animals show the normal sequence of arborization during all pupal stages examined (data not shown).

Expression of Gl^{Δ} reduces or abolishes GF–TTMn dye coupling

To begin to assess the function of the GF–TTM synapse in mutant animals, we examined dye coupling between the TTM and GF. These two neurons are known to be dye-coupled in wild type (Phelan et al., 1996), and we therefore iontophoresed dye into the TTMn and looked for coupling to the GF. To observe the adult morphology of the TTM neuron, and to test for connections with other cells, we backfilled the neuron from the TTM with neurobiotin. The control TTM was as described previously (Swain et al., 1990). The motorneuron shows a large, lateral cell body and three large characteristic processes: a medial dendrite, a posterior dendrite, and an axon that exits the CNS via the anterior dorsal medial nerve (Fig. 4*A*). The mutant (Gl^1/+) and transgenic (Gl^{Δ}) TTM neurons were not distinguishable from the wild type. In all specimens tested, the medial dendrite appeared normal and was in the correct position to be in close apposition to the GF terminal.

Table 2. Dye coupling between the TTMn and GF

Genotype	TTMns[a]	GFs filled	% coupled
Controls[b]	26	23	88
w; +/+; Gl^1/*TM6B*	14	13	93
w; c17/UAS–Gl^{Δ}	17	13	76
w; A307/UAS–Gl^{Δ}	12	3	25
Shaking B^2	12	0	0

[a]Only those specimens that showed heavy TTMn staining could be satisfactorily scored.

[b]Controls were P[GAL4] element alone (18 specimens) and *w*, Biocore (eight specimens); we observed no difference between the groups, and therefore they are combined.

Neurobiotin was seen to move from the TTM into the GF in a manner correlated with the presumed expression levels of the truncated Glued protein (Table 2). Preparations were scored for dye coupling to the GF (Fig. 4*A*,*B*, *arrows*) in a double-blind procedure (see Materials and Methods). The stained axon could be confirmed as the GF by following the neuron back up to the connective where the axon is easily identifiable. The apparent thinness of the giant axon therefore appears to be an artifact of the retrograde filling procedure. In wild-type specimens, coupling between TTM and the GF was often (90%) observed. In Gl^1/+ heterozygotes the dye traveled into the GF in >90% of the specimens (Fig. 4*A*), which was similar to the results for control specimens (88%, Table 2) (see also Phelan et al., 1996). In those specimens where Gl^{Δ} was expressed under control of the

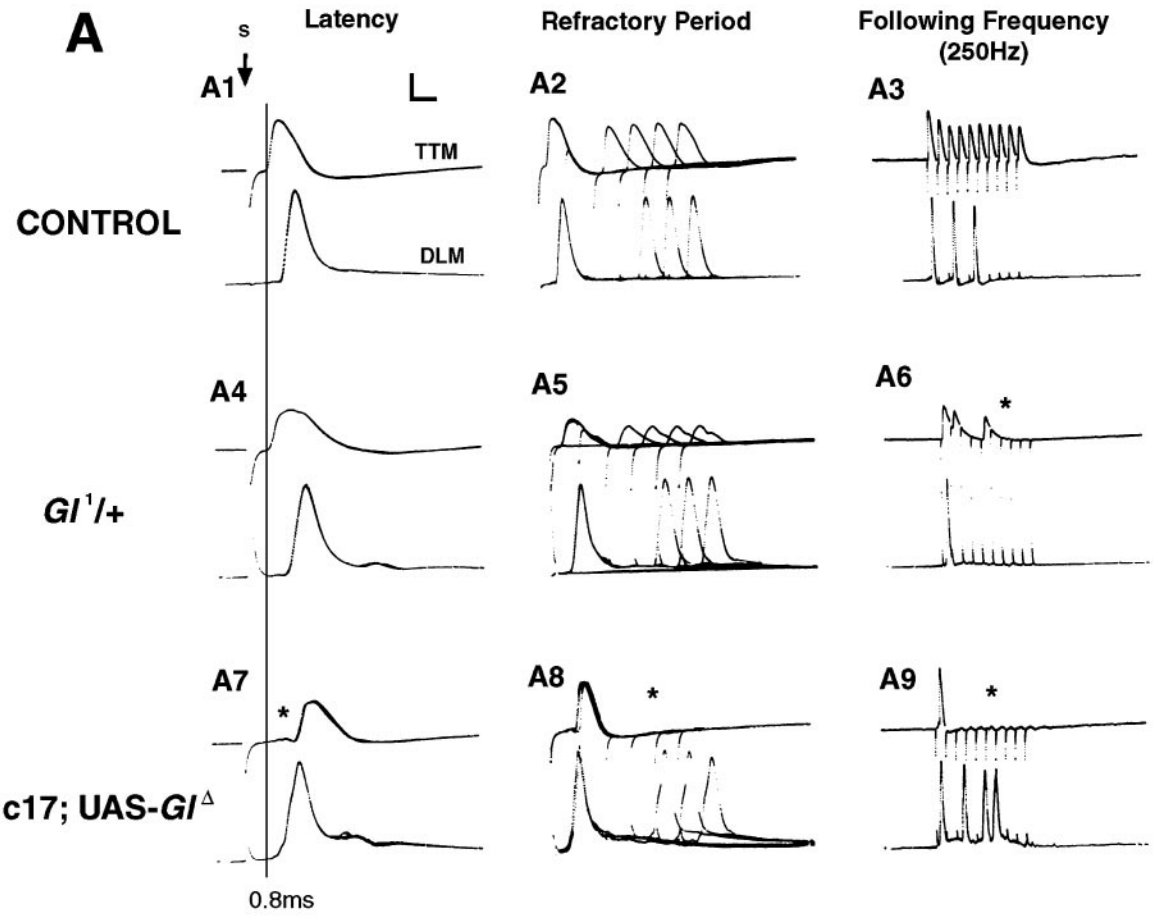

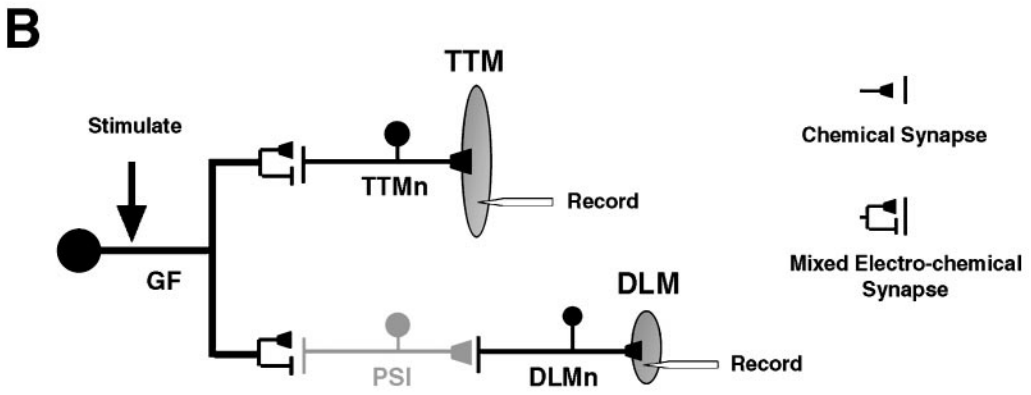

Figure 5. The Glued poison subunit disrupts the physiology of the giant fiber system. *A*, Recordings from individual control (*A1–3*), *Glued*^{1} (*A4–6*), and c17; UAS-*Gl*$^{\Delta 96B}$ (*A7–9*) animals. *A1*, *A*4, *A8*, The latency for wild type is indicated in *A1*, the beginning of stimulus is indicated by the *S*, and the *vertical line* represents the wild-type response latency for TTM (0.8 msec) and is drawn through all recordings for comparison. The longer TTM latency seen when the poison subunit was driven in the GF is highlighted with an *asterisk* in *A7*. Note that the disynaptic pathway to DLM remains constant in all three genotypes (~1.4 msec). Five responses are overlapped in each frame. *A2*, *A5*, *A8*, To determine the refractory period, twin stimuli were given with a different interstimulus interval (ISI) between the two (see Materials and Methods). Five different ISI responses are shown overlaid for each genotype with latencies of 10, 8, 6, 4, and 2 msec. A response to the first stimulation is always seen, and the minimal refractory period for TTM is 4 msec in controls, as well as in *Gl*^{1}/+. No second response is seen at any of these frequencies in the c17; UAS-*Gl*$^{\Delta}$ specimens (*A8*, *asterisk*). *A3*, *A6*, *A9*, For following frequency, a single sweep of 10 stimuli with an ISI of 4 msec is shown. In the wild-type animals, the TTM follows 1:1 (*A6*, *), but in the *Gl*^{1}/+ heterozygote and in the transgenic c17 animals no repetitive firing occurs (*A9*, *) Calibration: vertical scale bar, 20 mV for all traces; horizontal, 1 msec for *Latency*, 2 msec for *Refractory Period*, and 10 msec for *Following Frequency* (250 Hz). *B*, Schematic representing the identified neurons of the giant fiber system. Brain stimulation activates the GF, which in turn activates two follower neurons in the thorax: the tergotrochanteral motorneuron (*TTMn*) and the peripherally synapsing interneuron (*PSI*). The GF drives the tergotrochanteral muscle (*TTM*) through a monosynaptic pathway (*GF–TTMn*) and the flight muscles (*DLMs*) through a disynaptic pathway (*GF–PSI–DLMns*). Responses were recorded intracellularly from the TTM and a DLM.

Table 3. Synaptic function in wild-type and mutant specimens

	TTM				DLM		
Genotype	*n*	Latency (msec) ± SD	Refractory period (msec)	Following frequency (250 Hz)	Latency (msec) ± SD	Refractory period (msec)	Following frequency (250 Hz)
w; c17/*CyO*	7	0.83 ± 0.04	3.00	100%	1.42 ± 0.11	4.57	57.1%
w; A307/*CyO*	6	0.86 ± 0.10	4.17	88.3%	1.39 ± 0.14	4.67	55.0%
w; UAS–Gl^{Δ}/+;*TM6B*/+	6	0.73 ± 0.07	3.50	80.0%	1.33 ± 0.08	4.17	58.3%
w; +/+; Gl^{1}/*TM6B*	7	0.80 ± 0.04	4.14	42.9%	1.40 ± 0.11	5.00	28.6%
w; c17/UAS–Gl^{Δ}	11	1.36 ± 0.55	*a*	39.1%	1.53 ± 0.20	5.00	60.0%
w; A307/UAS–Gl^{Δ}	8	2.38 ± 0.52	*a*	10.0%	2.33 ± 0.41	*a*	16.0%

[a]Animals had refractory periods >10 msec and therefore were not measured (see Materials and Methods).

enhancer-trap showing weaker expression (c17), the probability of dye coupling to the GF was 76%. Finally, when Gl^{Δ} was expressed under control of the strongest driver (A307), the number of specimens exhibiting dye coupling dropped dramatically to 25%. Figure 4*C* shows an example in which no dye coupling from the TTMn to the GF was observed. As a negative control we examined mutant *Shaking*B^{2} specimens, which lack gap junctions, and found no dye coupling to the GF (Table 2). In summary, the dye coupling suggested that truncated Glued was disrupting the gap junction component of the GF–TTM synapse.

Function of the giant fiber system is altered in flies expressing Gl^{Δ} and in *Glued* sup1 mutants

Synaptic transmission at the GF–TTMn connection was abnormal when $Gl^{\Delta 96B}$ was expressed in the GF, showing that overexpression of the Glued poison subunit disrupts the function of this synapse. Three characteristics were used to assess synaptic function: response latency, refractory period, and following frequency (see Materials and Methods). In control flies, containing the P[GAL4] element or the UAS–$Gl^{\Delta 96B}$ construct alone, the stereotypical responses previously characterized for wild type (Tanouye and Wyman, 1980; Thomas and Wyman, 1982; Gorczyca and Hall, 1984) were seen; for TTM the latency is ~0.8 msec (Fig. 5*A1*), for refractory period 3–4 msec (Fig. 5*A2*), and for following frequency 80–100% at 250 Hz (Fig. 5*A3*). The DLM responses showed the characteristically longer latency (~1.4 msec) of the disynaptic pathway (Fig. 5*A1*), a correspondingly longer refractory period of >4 msec (Fig. 5*A2*), and poor following at 250 Hz (Fig. 5*A3*). Figure 5*A* shows sample recordings from individuals, and pooled data are shown in Table 3.

We found that the severity of the physiological phenotype correlated with expression levels, and they will be discussed in ascending order of levels of expression. Heterozygous Gl^{1}/+ flies showed the least effect and had a normal TTM response latency (0.8 msec) (Fig. 5*A4*) and refractory period (3–4 msec) (Fig. 5*A5*). However, repetitive stimulation resulted in TTM response failures at 250 Hz (Fig. 5*A6*, *asterisk*). This resulted in an average following frequency of only 42.9% (Table 3). When $Gl^{\Delta 96B}$ was expressed only presynaptically using c17, the adults showed changes in all three parameters in TTM (Fig. 5*A7–9*). Individual flies showed variable TTM latencies ranging from wild type (0.8 msec) to very long (>2 msec) (Fig. 5*A7*, *asterisk*), with a mean of 1.36 msec. The refractory period was >10 msec (Fig. 5*B8*, *asterisk*), and the TTM followed at 250 Hz with <40% reliability (Fig. 5*B9*, *asterisk*). In contrast, DLM muscle response remained normal in all specimens (Fig. 5*B7–9*, Table 3). This normal DLM response was unexpected because a structural study of Blagburn et al. (1999) shows the GF–PSI synapse to be mixed in nature and very similar to the GF–TTMn synapse. Interestingly, the *bendless* mutation shows a similar phenotype, with a longer TTM response latency and no effect on the GF–PSI–DLMn pathway (Thomas and Wyman, 1984). Our results therefore suggest that *Glued* may be involved in the same synaptic process, and we are currently looking for genetic interactions between $Glued^{1}$ and *bendless*.

When Gl^{Δ} was expressed using our strongest expressing line, A307, all adults tested showed altered physiology, and some exhibited no response at all (Fig. 6). Those flies that did respond showed longer latencies (χ = 2.38 msec) (Fig. 6*A1*, *asterisk*) and reduced following frequency (Fig. 6*A2*, Table 3). Direct stimulation of the thoracic ganglia, bypassing the GF, in the same preparation resulted in reversion of the TTM to a short latency of 0.7 msec (Tanouye and Wyman, 1980) (Fig. 6*A3*, *asterisk*) and high frequency after TTMn (Fig. 6*A4*). This direct stimulation of T2 showed that the TTMn neuromuscular junction was intact and that the defect was in the GF–TTMn synapse. Several of the A307; UAS–Gl^{Δ} flies that were tested gave no response in the TTM after brain stimulation (Fig. 6*B1*, *asterisk*). When the motorneuron was then stimulated directly in the same preparation, the TTM response was normal (Fig. 6*B2*). The failed response reflects the most extreme defect caused by the Gl^{Δ} protein in the giant fiber system; the GF–TTMn synapse was below threshold. The latency of the DLM was longer than wild type in all preparations (χ = 2.33 msec) (Fig. 6). Interestingly, it remained long (>1.5 msec) on direct stimulation, indicating that the motoneurons were affected (Fig. 6*A3*,*B1*,*B2*, *asterisks*). A307 shows expression in many motoneurons and therefore probably drives the poison subunit in the DLMns that could affect the neuromuscular junctions. A307 also shows expression in the TTMn (Allen et al., 1998), but antibody staining is weak, and we therefore presume that TTMn is unaffected because it expresses a low level of Gl^{Δ}.

Does $Glued^{1}$ affect chemical synaptic transmission?

The results shown in Figures 5 and 6 indicate that repetitive firing causes the GF–TTM synapse to fail at high (>100 Hz) frequencies in Gl^{1}/+ animals. The Gl^{1}/+ mutants have normal response latencies (χ = 0.80 msec) (Table 3) and refractory periods (χ = 4.14 msec) (Table 3) but a reduction in following at 250 Hz stimulation (Fig. 5, Table 3). The adult TTMn neuromuscular junction is very stable because muscle responses were seen even at 500 Hz on direct stimulation of the motorneuron (data not shown). We therefore interpret lack of a muscle response at 250 Hz as a failure of TTMn to reach threshold. Any depression at the

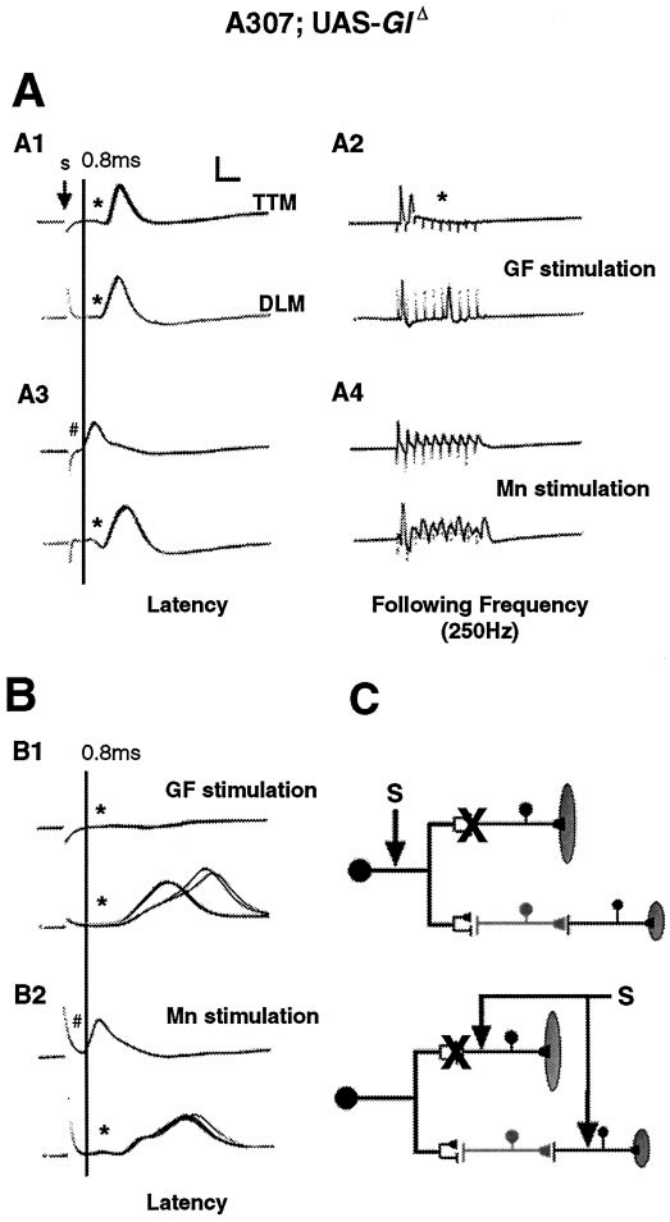

Figure 6. Strong expression of the Glued poison subunit weakens or abolishes the GF–TTMn synapse but not the neuromuscular junction. *A*, An experimental A307; UAS–$Gl^{\Delta 96B}$ specimen with a weakened synapse. The latency of the TTM synapse is longer that normal (*A1*, *), and the following frequency is much lower than normal (*A2*, *). When the motor neurons were stimulated directly, the latency of the TTM response was restored to a very short latency of 0.7 msec (*A3*, *B2*, #), showing that the TTMn and its neuromuscular junction are normal and the defect can be attributed to the GF–TTMn synapse. *B*, Some specimens exhibit no TTM response. In this specimen there was never a TTM response to GF stimulation (*B1*, *top trace asterisk*). B2 shows that direct stimulation can still activate the TTMn and its neuromuscular junction. *C*, Schematic representing the methods of stimulation to test for a weakened or absent GF–TTMn synapse. Calibration: vertical scale bar, 20 mV for all traces; horizontal, 1 msec for *Latency* and 10 msec for *Following Frequency* (250 Hz).

synapse would therefore be revealed by a lack of muscle response as the probability of reaching threshold decreased.

To assess the repetitive firing more accurately, we tested each animal with 10 bouts of 10 pulses at various frequencies. The results for control (Canton-S) animals are shown in Figure 7*A*. At 100 Hz, the wild-type specimens show almost no response decrement and respond to nearly every stimulus, responding 9 of 10 times by the end of the series of 10 stimuli. As the frequency is increased to 200 and 300 Hz, a clear response decrement or depression is recorded, with the plateau at ~70% for 200 Hz and near the 60% level at 300 Hz. In contrast, when heterozygous $Gl^1/+$ specimens are tested, they exhibit more rapid depression curves and lower plateaus (Fig. 7*B*). At 200 Hz the plateau is at 50% responsiveness, and at 300 Hz it is at 30% responsiveness. These curves of response decrement are reminiscent of depression at a chemical synapse and suggest that the Gl^1 mutation is disrupting the function of a chemical synapse.

At 300 Hz, a clear dip in responsiveness was recorded at the second stimulus, but the remainder of the curve appears to follow the exponential normally seen for depression at chemical synapses. This unresponsiveness to the second stimulation is highly reliable throughout our experiments, although it has not been described previously. We assume it is caused by activation of a local inhibitory pathway but have not examined it further.

The observed response curves indicate that the GF–TTMn synapse is depressing in a manner similar to chemical synapses (Hill and Jin, 1998). We therefore targeted expression of tetanus toxin to the GFs using line c17. This toxin inhibits chemical transmission in *Drosophila* by cleaving synaptobrevin and thus preventing evoked transmitter release (Sweeney et al., 1995). Specimens with targeted expression of tetanus toxin show normal latencies and refractory periods but exhibit more rapid response decrement (Fig. 7*D*) than the genetic controls (Fig. 7*C*) or the Canton-S control (Fig. 7*A*). This result strongly suggests that a component of the GF–TTM synapse is chemical and that it is being inhibited but not abolished by the toxin. Equally important, the tetanus toxin-treated specimens are very similar to the $Gl^1/+$ heterozygotes, suggesting that *Glued*^{1} is disrupting a chemical component of the synapse.

DISCUSSION

By targeting the expression of truncated Glued protein to the giant fiber system, we have demonstrated that the retrograde motor is needed to build a normal synaptic connection between two identified neurons in the *Drosophila* CNS. In transgenic specimens expressing a truncated version of the p150 subunit of the dynein–dynactin complex, GF axons show normal growth and pathfinding out of the brain and into the thoracic ganglia where they stop at their normal contact points. However, the GF fails to develop a normal presynaptic terminal bend, the axon terminal becomes clogged with large vesicles, and the terminal swells to several times the normal axon diameter. Depending on dosage of the mutant protein, these GFs make either very weak or no detectable synaptic connection with the TTMn. In the transgenic animals, where we think the truncated protein is expressed at the highest levels (A307), the specimens show the most severe swelling of the presynaptic terminal, and as measured physiologically, often completely lack a synaptic connection and often exhibit no dye coupling to the TTMn. In $Gl^1/+$ mutants, which appear to express the lowest amount of truncated protein, a morphologically normal presynaptic terminal is assembled, and dye coupling appears normal but synaptic function is compromised. The physiological effects seen in the $Gl^1/+$ specimens, normal latencies but very poor response to repetitive firing, is reproduced by expressing the tetanus toxin light chain in the GFs. This suggests that the chemical component of the synapse is more sensitive to low levels of the poison subunit. Normal assembly of both the gap junctional

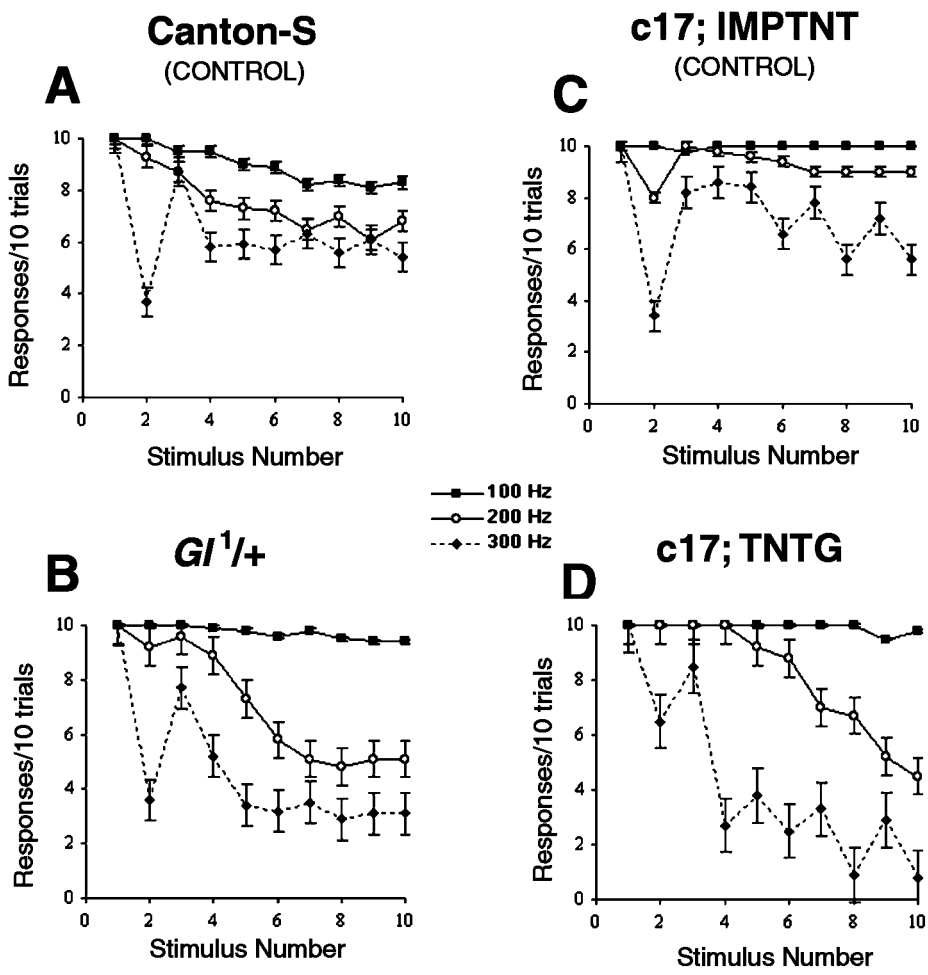

Figure 7. *Glued*[1] mutation compromises the chemical component of the GF–TTMn synapse. *A*, The response of a control TTM to repetitive GF stimulation at three frequencies. *B*, The response of the TTM to repetitive firing of the GF in a Gl^1/+ specimen. Note the strong depression at 200 and 300 Hz. *C*, Driving the defective version of the tetanus toxin transgene has no affect on repetitive firing. *D*, Expression of the tetanus toxin light chain in the GF reduces the response to repetitive firing. Note the similarity between these curves and the Gl^1/+ heterozygotes.

component and the chemical component of the mixed synaptic connection is therefore dependent on the normality of function of the dynactin complex.

Development of the synapse

The defect in GF bending is first seen at 48 hr APF, and the appearance of large vesicles and swelling of the axon terminal begin at about this time. GF–TTM contact in specimens has been made before the time that these anatomical defects appear. Previous work at the light microscope level suggested that the GF and TTMn have made anatomical contact by 24 hr APF, and GF bending occurs before 48 hr APF (Allen et al., 1998). In addition, dye injection of the GF axon has shown it to be dye-coupled to the TTMn by 45 hr APF (Phelan et al., 1996).

We presume that the swelling of the GF is caused by accumulation of transport vesicles at the distal tip of the axons, because the GFs have stopped elongating and are unable to perform normal dynein–dynactin-mediated retrograde transport, and material accumulates in the axon terminal. Disruption of retrograde transport leads to swellings only in the distal axons and occurs only after the axon has reached the target region. This may reflect the fact that little dynein–dynactin retrograde transport is needed during rapid axonal outgrowth and becomes crucial only after the axons stops growing. Experiments with cultured chick sympathetic neurons show a fourfold increase in retrograde transport of organelles when axon extension is blocked (Hollenbeck and Bray, 1987). In contrast, in kinesin mutants the organelle jams occur spaced along the length of the axons (Hurd and Saxton, 1996). We have looked at flies that express Gl^{Δ} in the GFs in a Gl^1 background and thus have a very high level of truncated Glued; these flies show more severe defects in which large vesicles can be seen along the length of the GFs (data not shown). This indicates that more severe disruption of the retrograde machinery may lead to swellings closer to the cell body.

The GFs in Gl^1/+ heterozygotes show normal anatomy at the light microscope level. We presume that there are sufficient wild-type dynein–dynactin complexes to enable synaptogenesis to occur correctly. Our previous analysis of sensory neurons in Gl^1 mutants shows defects in axon trajectory (Reddy et al., 1997; Murphey et al., 1999). However, when Gl^{Δ} is targeted to these sensory neurons, pathfinding and trajectory are normal, but the axon bundles show varicosities where they make synaptic contacts (M. J. Allen, unpublished data). This is consistent with the results presented here and suggests that the pathfinding defects seen in the sensory neurons of *Glued* [1] animals are attributable to abnormalities in the neuropil in which they are growing.

Models for synapse assembly and maturation

The results suggest two possible mechanisms that are not mutually exclusive. On the one hand, the dynein–dynactin system may be required for local cytoskeletal rearrangements that are necessary in the axon to create the large presynaptic terminal of the GF. On the other hand, the retrograde motor may be required for long distance signaling to the nucleus to activate gene expression that is required for synapse maturation.

One of the distinguishing characteristics of the GF is the large

presynaptic region adjacent to the TTM dendrite (Blagburn et al., 1999). This unusual structure suggests that local cytoskeletal rearrangements may be required for correct formation of this enlarged presynaptic terminal bend. Recent evidence suggests a role for the retrograde motor machinery in the transport of microtubules in an anterograde direction (Ahmad et al., 1998; Baas, 1999). This might be achieved when the cargo-binding end of the dynein–dynactin complex is anchored in the actin matrix, and thus ATP activation will cause the microtubule to be propelled in an anterograde direction. This is proposed as a mechanism for pushing microtubules into extending growth cones during neurite extension (Baas, 1999). The data presented here do not support a general role for dynein–dynactin in axonal outgrowth because the defective GFs show normal axonal outgrowth and normal arborization of the dendrites. However, the movement of microtubules may be involved in more specific growth and rearrangement of the cytoskeleton that is needed as the GF extends along the TTMn to make synaptic contact in the terminal phases of synaptogenesis. A related possibility is that the membrane accumulations that occur in the transgenic animals prevent the normal assembly of the terminal cytoskeleton as the axon enlarges and bends along the TTM dendrite.

A second possibility is that the retrograde motor carries a signal from the axon tip back to the cell body where gene activation is required for the GF–TTMn synapse to mature. Synaptogenesis and synapse maturation require bidirectional communication between the synaptic partners (Davis and Murphey, 1994) as well as bidirectional communication between synapse and soma within a neuron, and molecular motors are crucial to the intracellular processes (Brady, 1991; Tanaka and Sabry, 1995). The TTMn might express a trophic signal on its surface, which is endocytosed by the GF and transported back to the soma where transcription is activated, and the gene products that are synthesized lead to synapse maturation. By expressing Gl^{Δ} in the GF, we have disabled the retrograde machinery and prevented or reduced the amount of the putative signal reaching the cell body. This lack of modulation of gene expression might then cause a failure in maturation of the synapse with TTMn.

We cannot distinguish between a local modulation of the cytoskeleton and long distance modulation of gene expression, and both may be involved. The models we propose are very close to the models for classical retrograde signals, such as nerve growth factor (NGF). Some of NGF's effects depend on the retrograde movement of the NGF–TrkA receptor complex from synapse to soma, whereas others are much more local and affect axon terminal growth without reference to the nucleus (Campenot, 1994).) There is relatively little evidence for NGF or its receptor in *Drosophila* (Hayashi et al., 1992; Wilson et al., 1993), and we are currently testing other candidate molecules that have the requisite properties to play the neurotrophic role in *Drosophila*.

Nature of the GF synapses

Recently Blagburn et al. (1999) used electron microscopy to investigate the nature of the GF–TTMn synapse in wild-type and $Shaking B^2$ mutants (that lack gap junctions) and showed the presence of vesicles and other features of a chemical synaptic transmission. Our data support these findings because expression of tetanus toxin lowered the reliability of the synapse in a manner consistent with weakening chemical transmission. We were surprised to observe these effects, because it has always been assumed that the tight electrical coupling between GF and TTMn was sufficient to drive the synapse at high frequencies. Our results suggest the contrary: the chemical component is important for normal repetitive function. The dose-dependent responses of the GF leave open the possibility of acute effects on membrane recycling or transmitter release.

Because Blagburn et al. (1999) revealed that both GF–TTMn and GF–PSI were mixed synapses, the differential effect of Gl^{Δ} on these two synapses is surprising and indicates that there are differences between the two. This could be attributable to the proportions of the electrical and chemical components. The GF–TTMn pathway may be more dependent on chemical transmission than GF–PSI. Interestingly, *Shaking* B^2 (*passover*) mutants show no GF–PSI–DLMn pathway when tested electrophysiologically (Thomas and Wyman, 1984), indicating that it is heavily reliant on gap junctions but a long-latency GF–TTMn pathway, suggesting the possibility of a remaining chemical component.

REFERENCES

Adams JC (1981) Heavy metal intensification of DAB-based HRP reaction product. J Histochem Cytochem 29:775.

Ahmad FJ, Echeverri CJ, Vallee RB, Baas PW (1998) Cytoplasmic dynein and dynactin are required for the transport of microtubules into the axon. J Cell Biol 140:391–401.

Allan V (1996) Motor proteins: a dynamic duo. Curr Biol 6:630–633.

Allen MJ, Drummond JA, Moffat KG (1998) Development of the giant fiber neuron of *Drosophila* melanogaster. J Comp Neurol 397:519–531.

Baas PW (1999) Microtubules and neuronal polarity: lessons from mitosis. Neuron 22:23–31.

Bainbridge SP, Bownes M (1981) Staging the metamorphosis of *Drosophila* melanogaster. J Embryol Exp Morphol 66:57–80.

Basler K, Siegrist P, Hafen E (1989) The spatial and temporal expression pattern of sevenless is exclusively controlled by gene-internal elements. EMBO J 8:2381–2386.

Blagburn JM, Alexopoulos H, Davies JA, Bacon JP (1999) Null mutation in shaking-B eliminates electrical, but not chemical, synapses in the *Drosophila* giant fiber system: a structural study. J Comp Neurol 404:449–458.

Brady ST (1991) Molecular motors in the nervous system. Neuron 7:521–533.

Brand AH, Perrimon N (1993) Targeted gene-expression as a means of altering cell fates and generating dominant phenotypes. Development 118:401–415.

Campenot RB (1994) NGF and the local control of nerve terminal growth. J Neurobiol 25:599–611.

Davis GW, Murphey RK (1994) Long-term regulation of short-term release properties: retrograde signaling and synaptic development. Trends Neurosci 17:9–13.

Engel JE, Wu CF (1996) Altered habituation of an identified escape circuit in *Drosophila* memory mutants. J Neurosci 16:3486–3499.

Fan SS, Ready DF (1997) Glued participates in distinct microtubule-based activities in *Drosophila* eye development. Development 124:1497–1507.

Freeman M (1996) Reiterative use of the EGF receptor triggers differentiation of all cell types in the *Drosophila* eye. Cell 87:651–660.

Gho M, McDonald K, Ganetzky B, Saxton WM (1992) Effects of kinesin mutations on neuronal functions. Science 258:313–316.

Gindhart Jr JG, Desai CJ, Beushausen S, Zinn K, Goldstein LS (1998) Kinesin light chains are essential for axonal transport in *Drosophila*. J Cell Biol 141:443–454.

Gorczyca M, Hall JC (1984) Identification of a cholinergic synapse in the giant fiber pathway of *Drosophila* using conditional mutations of acetylcholine synthesis. J Neurogenet 1:289–313.

Harte PJ, Kankel DR (1983) Analysis of visual system development in *Drosophila* melanogaster: mutations at the Glued locus. Dev Biol 99:88–102.

Hayashi I, Perez-Magallanes M, Rossi JM (1992) Neurotrophic factor-like activity in *Drosophila*. Biochem Biophys Res Commun 184:73–79.

Hill AA, Jin P (1998) Regulation of synaptic depression rates in the cricket cercal sensory system. J Neurophysiol 79:1277–1285.

Hirokawa N (1998) Kinesin and dynein superfamily proteins and the mechanism of organelle transport. Science 279:519–526.

Hollenbeck PJ, Bray D (1987) Rapidly transported organelles containing membrane and cytoskeletal components: their relation to axonal growth. J Cell Biol 105:2827–2835.

Holleran EA, Karki S, Holzbaur EL (1998) The role of the dynactin complex in intracellular motility. Int Rev Cytol 182:69–109.

Hurd DD, Saxton WM (1996) Kinesin mutations cause motor neuron disease phenotypes by disrupting fast axonal transport in *Drosophila*. Genetics 144:1075–1085.

Hurd DD, Stern M, Saxton WM (1996) Mutation of the axonal transport motor kinesin enhances paralytic and suppresses Shaker in *Drosophila*. Genetics 142:195–204.

Karki S, Holzbaur ELF (1995) Affinity-chromatography demonstrates a direct binding between cytoplasmic dynein and the dynactin complex. J Biol Chem 270:28806–28811.

King DG, Wyman RJ (1980) Anatomy of the giant fiber pathway in *Drosophila.* I. Three thoracic components of the pathway. J Neurocytol 9:753–770.

McGrail M, Gepner J, Silvanovich A, Ludmann S, Serr M, Hays TS (1995) Regulation of cytoplasmic dynein function in-vivo by the *Drosophila* Glued complex. J Cell Biol 131:411–425.

Murphey RK, Caruccio P, Getzinger M, Westgate PJ, Phillis RW (1999) Dynein–dynactin function and sensory axon growth during *Drosophila* metamorphosis: a role for retrograde motors. Dev Biol 209:86–97.

Phelan P, Nakagawa M, Wilkin MB, Moffat KG, O'Kane CJ, Davies JA, Bacon JP (1996) Mutations in shaking-B prevent electrical synapse formation in the *Drosophila* giant fiber system. J Neurosci 16:1101–1113.

Phillis R, Statton D, Caruccio P, Murphey RK (1996) Mutations in the 8 kDa dynein light-chain gene disrupt sensory axon projections in the *Drosophila* imaginal CNS. Development 122:2955–2963.

Reddy S, Jin P, Trimarchi J, Caruccio P, Phillis RW, Murphey RK (1997) Mutant molecular motors disrupt neural circuits in *Drosophila*. J Neurobiol 33:711–723.

Riccio A, Pierchala BA, Ciarallo CL, Ginty DD (1997) An NGF-TrkA-mediated retrograde signal to transcription factor CREB in sympathetic neurons. Science 277:1097–1100.

Spradling AC, Rubin GM (1983) The effect of chromosomal position on the expression of the *Drosophila* xanthine dehydrogenase gene. Cell 34:47–57.

Swain GP, Wyman RJ, Egger MD (1990) A deficiency chromosome in *Drosophila* alters neuritic projections in an identified motoneuron. Brain Res 535:147–150.

Swaroop A, Paco-Larson ML, Garen A (1985) Molecular genetics of a transposon-induced dominant mutation in the *Drosophila* locus Glued. Proc Natl Acad Sci USA 82:1751–1755.

Sweeney ST, Broadie K, Keane J, Niemann H, O'Kane CJ (1995) Targeted expression of tetanus toxin light-chain in *Drosophila* specifically eliminates synaptic transmission and causes behavioral defects. Neuron 14:341–351.

Tanaka E, Sabry J (1995) Making the connection: cytoskeletal rearrangements during growth cone guidance. Cell 83:171–176.

Tanouye MA, Wyman RJ (1980) Motor outputs of giant nerve fiber in *Drosophila*. J Neurophysiol 44:405–421.

Thomas JB, Wyman RJ (1982) A mutation in *Drosophila* alters normal connectivity between two identified neurons. Nature 298:650–651.

Thomas JB, Wyman RJ (1983) Normal and mutant connectivity between identified neurons in *Drosophila*. Trends Neurosci 6:214–219.

Thomas JB, Wyman RJ (1984) Mutations altering synaptic connectivity between identified neurons in *Drosophila*. J Neurosci 4:530–538.

Trimarchi JR, Murphey RK (1997) The shaking-B2 mutation disrupts electrical synapses in a flight circuit in adult *Drosophila*. J Neurosci 17:4700–4710.

Trimarchi JR, Schneiderman AM (1994) The motor neurons innervating the direct flight muscles of *Drosophila melanogaster* are morphologically specialized. J Comp Neurol 340:427–443.

Trimarchi JR, Jin P, Murphey RK (1999) Controlling the motor neuron. Int Rev Neurobiol 43:241–264.

Vaughan KT, Vallee RB (1995) Cytoplasmic dynein binds dynactin through a direct interaction between the intermediate chains and Pl50(Glued). J Cell Biol 131:1507–1516.

Waterman-Storer CM, Holzbaur ELF (1996) The product of the *Drosophila* gene, *Glued*, is the functional homolog of the P150(Glued) component of the vertebrate dynactin complex. J Biol Chem 271:1153–1159.

Waterman-Storer CM, Karki SB, Kuznetsov SA, Tabb JS, Weiss DG, Langford GM, Holzbaur EL (1997) The interaction between cytoplasmic dynein and dynactin is required for fast axonal transport. Proc Natl Acad Sci USA 94:12180–12185.

Wilson C, Goberdhan DCI, Stellar H (1993) Dror, a potential neurotrophic receptor gene, encodes a *Drosophila* homolog of the vertebrate Ror family of Trk-related receptor tyrosine kinases. Proc Natl Acad USA 90:7109–7113.